Global drivers of obligate mycorrhizal symbionts diversification

Benoît Perez-Lamarque [1,2 *], Maarja Öpik [3], Odile Maliet [1], Ana C. Afonso Silva [1], Marc-André Selosse [2,4], Florent Martos [2], and Hélène Morlon [1]

[1] *Institut de biologie de l'École normale supérieure (IBENS), École normale supérieure, CNRS, INSERM, Université PSL, 46 rue d'Ulm, 75 005 Paris, France*

[2] *Institut de Systématique, Évolution, Biodiversité (ISYEB), Muséum national d'histoire naturelle, CNRS, Sorbonne Université, EPHE, UA, CP39, 57 rue Cuvier 75 005 Paris, France*

[3] *University of Tartu, 40 Lai Street, 51 005 Tartu, Estonia*

[4] *Department of Plant Taxonomy and Nature Conservation, University of Gdansk, Wita Stwosza 59, 80-308 Gdansk, Poland*

* *corresponding author: benoit.perez@ens.psl.eu; ORCID:* 0000-0001-7112-7197

Abstract (200 words):

Arbuscular mycorrhizal fungi (AMF) are widespread microscopic fungi that provide mineral nutrients to most land plants by forming one of the oldest terrestrial symbioses. They have sometimes been referred to as an "evolutionary cul-de-sac" for their limited species diversity and their ecological niches restricted to plant-symbiotic life style. Here we use the largest global database of AMF to analyze their diversification dynamics in the past 500 million years (Myr) based on the small subunit (SSU) rRNA gene. We demonstrate that overall the SSU rRNA gene is variable enough to delineate AMF species and find that AMF have low diversification rates. After a diversification peak around 150 Myr ago, they experienced an important diversification slowdown in the last 100 Myr, likely related to a shrinking of their mycorrhizal niches. Our results identify patterns and drivers of diversification in a group of obligate symbionts of major ecological and evolutionary importance. They also highlight a striking example of a diversification slowdown that, instead of reflecting an adaptive radiation as typically assumed, may result from a limited ability to colonize new niches in an evolutionary cul-de-sac.

Introduction:

Arbuscular mycorrhizal fungi (AMF - subphylum Glomeromycotina) are obligate symbionts sometimes referred to as an "evolutionary cul-de-sac, albeit an enormously successful one" [1, 2]. They have limited morphological and species diversities, yet associate with the roots of >80% of land plants, where they provide mineral resources in exchange for photosynthates [3]. Present in most terrestrial ecosystems, AMF play key roles in plant protection, nutrient cycling, and ecosystem functions [4]. Fossil evidence and molecular phylogenies suggest that AMF contributed to the emergence of land plants [5–8] and coevolved with them for more than 400 million years (Myr)[8–10].

Despite the ecological ubiquity and evolutionary importance of AMF, large-scale patterns of their evolutionary history are poorly known. Studies on the diversification of AMF have been hampered by the difficulty of delineating species, quantifying global scale species richness, and building a robust phylogenetic tree for this group. Indeed, AMF are microscopic soil- and root-dwelling fungi that are poorly differentiated morphologically and difficult to cultivate. Although their classical taxonomy is mostly based on the characters of spores and root colonization [3, 11], AMF species delineation has greatly benefited from molecular data [12]. Experts have defined "virtual taxa" (VT) based on a minimal 97% similarity of a region of the 18S small subunit (SSU) rRNA gene and monophyly criteria [13, 14]. As for many other pragmatic species concepts, VT have rarely been tested for their biological relevance [15], and a consensual system of AMF classification is still lacking [16]. AMF are also poorly known genetically: the full SSU rRNA gene sequence is known in few species [17], other gene sequences in even fewer [10, 18], and complete genomes in very few [19].

The drivers of AMF diversification are unknown. A previous dated phylogenetic tree of VT found that many speciations occurred after the last major continental reconfiguration around 100 Myr ago [20], suggesting that AMF diversification is not linked to vicariant speciation during this geological event. Still, geographical speciation could play an important role in AMF diversification, as these organisms have spores that disperse

efficiently [21–23], which could result in frequent founder-event speciation [24]. Other abiotic factors include habitat: tropical grasslands have, for example, been suggested as diversification hotspots for AMF [25]. Besides abiotic factors, AMF are obligate symbionts and, although relatively generalist [4, 26, 27], their evolutionary history could be largely influenced by a diffuse coevolution with their host plants [10, 28, 29]. Over the last 400 Myr, land plants have experienced massive extinctions and radiations [29, 30], adaptations to various ecosystems [31, 32], and associations with different soil microorganisms [33, 34]. All these factors could have influenced diversification dynamics in AMF.

Here, we reconstruct several thoroughly sampled phylogenetic trees of AMF, considering several criteria of species delineations and uncertainty in phylogenetic reconstructions. We combine this phylogenetic data with paleoenvironmental data and data of current AMF geographic distributions, ecological traits, interaction with host plants, and genetic diversity to investigate the global patterns and drivers of AMF diversification in the last 500 Myr.

Material & methods:

Database choice:

We used AMF SSU rRNA gene sequences from MaarjAM database, the largest global database of AMF gene sequences [13]. Ideally, our analyses would be based on several independent genomic regions, however such data has yet to be acquired. In fungi, the usual barcode is the ITS region. However, for several reasons the SSU rRNA gene has been preferred over the ITS in AMF [35], and therefore ITS data on AMF are currently less common. In addition, we confirmed using the dataset of [35] that the ITS are very difficult to align, preventing us from reconstructing a robust phylogeny to investigate AMF evolutionary history (Supplementary Fig. 1).

Virtual taxa phylogenetic reconstruction:

We reconstructed several Bayesian phylogenetic trees of the 384 VT from the corresponding representative sequences available in the MaarjAM database [13] updated in June 2019 (Supplementary Methods 1). We used the full length (1,700 base pairs) SSU rRNA gene sequences from [17] to better align the VT sequences using MAFFT [36]. We selected the 520 base pair central variable region of the VT aligned sequences and performed a Bayesian phylogenetic reconstruction using BEAST2 [37]. We obtained a consensus VT tree and selected 12 trees equally spaced in 4 independent Bayesian chains to account for phylogenetic uncertainty in the subsequent diversification analyses, hereafter referred to as the VT replicate trees. We set the crown root age at 505 Myr [20], which is coherent with fossil data and previous dated molecular phylogenies [8, 10].

Delineation into Evolutionary Units (EUs):

We considered several ways to delineate AMF species based on the SSU rRNA gene. In addition to the VT species proxy, we delineated AMF *de novo* into evolutionary units (EUs) using 5 different thresholds of sequence similarity ranging from 97 to 99% and a monophyly criterion. We gathered 36,411 AMF sequences of the SSU rRNA gene from MaarjAM, mainly amplified by the primer pair NS31–AML2 (variable region) [38, 39] (dataset 1, Supplementary Table 1), corresponding to 27,728 haplotypes. We first built a phylogenetic tree of these haplotypes and then applied to this tree our own algorithm (R-package RPANDA [40, 41]) that traverses the tree from the root to the tips, at every node computes the average similarity of all sequences descending from the node, and collapses the sequences into a single EU if their sequence dissimilarity is lower than a given threshold (Supplementary Methods 2). Finally, we performed Bayesian phylogenetic reconstructions of the EUs using BEAST2, following the procedure described in Supplementary Methods 1.

Coalescent-based species delineation analyses:

Finally, we considered the Generalized Mixed Yule Coalescent method (GMYC) [42, 43], a species delineation approach that does not require specifying an arbitrary similarity threshold. GMYC estimates the time t in a reconstructed calibrated tree that separates species diversification (Yule process – before t) and intraspecific differentiation (coalescent process – after t). GMYC is too computationally intensive to apply on the 36,411 SSU sequences; we used it here on three smaller clades to investigate the ability of the SSU gene to delineate AMF species despite its slow evolution [16], and as a way to evaluate the biological relevance of the VT and various EUs delineations. We selected the following AMF clades: the family Claroideoglomeraceae; the order Diversisporales; and an early-diverging clade composed of the orders Archaeosporales and Paraglomerales. For each clade, we reconstructed Bayesian phylogenetic trees of haplotypes following the procedure described in Supplementary Methods 1. We then ran GMYC analyses (splits R-package [44]) on each of these trees and evaluated the support of the GMYC model compared to a

null model in which all tips are assumed to be different species, using a likelihood ratio test (LRT). If the LRT supports the GMYC model, different SSU haplotypes belong to the same AMF species, *i.e.* the SSU rRNA gene has time to accumulate substitutions between AMF speciation events.

Total diversity estimates:

We evaluated how thoroughly sampled our species-level AMF phylogenetic trees are by estimating the total number of VT and EUs using rarefaction curves and the Bayesian Diversity Estimation Software (BDES [45]) (Supplementary Methods 3).

Diversification analyses:

We estimated lineage-specific diversification rates using ClaDS, a Bayesian diversification model that accounts for rate heterogeneity by modeling small rate shifts at speciation events [46]. At each speciation event, the descending lineages inherit new speciation rates sampled from a log-normal distribution with an expected value $\log[\alpha \times \lambda]$ (where λ represents the parental speciation rate and α is a trend parameter) and a standard deviation σ. We considered the model with constant turnover ε (*i.e.* constant ratio between extinction and speciation rates; *ClaDS2*) and ran a newly developed ClaDS algorithm based on data augmentation techniques which enables us to estimate mean rates through time (https://github.com/OdileMaliet/ClaDS_Julia). We ran ClaDS2 with 3 independent chains, checked their convergence using a Gelman-Rubin diagnostic criterion [47], and recorded lineage-specific speciation rates. We also recorded the estimated hyperparameters (α, σ, ε) and the value $m=\alpha \times \exp(\sigma^2/2)$, which indicates the general trend of the rate through time [46].

In addition, we applied TreePar [48], another diversification approach that does not consider rate variation across lineages, but models temporal shifts in diversification rates

163 affecting all lineages simultaneously. We searched for up to ten shifts in diversification
164 rates at every 2-million-year interval in each phylogenetic tree. We estimated the number
165 of temporal shifts in AMF diversification rates using maximum likelihood inferences and
166 likelihood ratio tests. We also used CoMET, its equivalent piecewise-constant model in a
167 Bayesian framework (TESS R-package [49, 50]). We chose the Bayesian priors according to
168 maximum likelihood estimates from TreePar, disallowed mass extinction events, and ran
169 the MCMC chains until convergence (minimum effective sample sizes of 500).
170
171 We also fitted a series of time-dependent and environment-dependent birth-death
172 diversification models using RPANDA [40, 51] to test the influence of temperature, pCO_2,
173 and land plant fossil diversity on AMF diversification. For the time-dependent models, we
174 considered models with constant or exponential variation of speciation rates through time
175 and null or constant extinction rates (*fit_bd* function). Models with constant rates
176 correspond to the null hypothesis of clock-like speciation, whereas the exponential
177 variation ensures positive rates and are an approximation of diversity dependence, a
178 process often invoked during radiations [52]. For the environment-dependent models, we
179 considered an exponential dependency of the speciation rates with the environmental
180 variable (env), *i.e.* speciation rate=b*exp(a*env), where a and b are two parameters
181 estimated by maximum likelihood (*fit_env* function). The exponential variation
182 corresponds here to a simple linear regression of log-transformed rates. Environment
183 curves were smoothed using the function *smooth.spline* (stats R-package). We used the
184 corrected Akaike information criterion (AICc) to select the best-fit models, considering that
185 a difference of 2 in AICc indicates that the model with the lowest AICc is better.
186 The influence of temperature was tested on the complete AMF phylogenetic trees,
187 using estimates of past global temperature [53]. As these temporal analyses can be sensitive
188 to the root age calibration, we replicated them using the youngest (437 Myr) and oldest
189 (530 Myr) crown age estimates from [10]. The influence of pCO_2 [54] and of land plant fossil
190 diversity was tested starting from 400 Myr ago, as these environmental data are not
191 available for more ancient times. For these analyses we sliced the phylogenies at 400 and

192 200 Myr ago, and applied the diversification models to the sliced sub-trees larger than 50
193 tips. Estimates of land plant diversity were obtained using all available Embryophyta
194 fossils from the Paleobiology database (https://paleobiodb.org) and using the shareholder
195 quorum subsampling method (Supplementary Methods 4; [55]).
196
197 All diversification analyses were performed for each delineation on the consensus
198 and on the 12 replicate trees to account for phylogenetic uncertainty. We also considered
199 missing species by imputing sampling fractions, computed as the number of observed VT
200 or EUs divided by the corresponding BDES estimates of global AMF diversity estimated
201 from Sichel distributions (Supplementary Table 2). As such analyses depend on diversity
202 estimates, we replicated all diversification analyses using lower sampling fractions down
203 to 50%.
204
205 **Testing for potential drivers of AMF diversification:**
206
207 To further investigate the potential factors driving AMF diversification, we assessed
208 the relationship between lineage-specific estimates of present-day speciation rates and
209 characteristics of each AMF taxonomic unit, *i.e.* VT or EUs.
210
211 First, we characterized AMF niche width using a set of 10 abiotic and biotic variables
212 recorded in MaarjAM database for each AMF unit. In short, among a curated dataset
213 containing AMF sequences occurring only in natural ecosystems (dataset 2; [26]), for each
214 AMF unit, we reported the number of continents, ecosystems, climatic zones,
215 biogeographic realms, habitats, and biomes where it was sampled, as well as its number of
216 plant partners, their phylogenetic diversity, and its centrality in the plant-fungus bipartite
217 network, and performed a principal component analysis (PCA; Supplementary Methods
218 5). For AMF units represented by at least 10 sequences, we tested whether these PCA
219 coordinates reflecting AMF niche widths were correlated with the present-day speciation
220 rates using both linear mixed-models (not accounting for AMF phylogeny) or

221 MCMCglmm models [56]. For MCMCglmm, we assumed a Gaussian residual distribution,
222 included the fungal phylogenetic tree as a random effect, and ran the MCMC chains for
223 1,300,000 iterations with a burn-in of 300,000 and a thinning interval of 500.
224
225 Next, we tested the relationship between speciation rates and geographic
226 characteristics of AMF units. To test the effect of latitude, we associated each AMF unit
227 with its set of latitudes and used similar MCMCglmm with an additional random effect
228 corresponding to the AMF unit. To account for inhomogeneous sampling along the
229 latitudinal gradient, we re-ran the model on jackknifed datasets (we re-sampled 1,000
230 interactions per slice of latitude of twenty degrees). Similarly, we tested the effect of
231 climatic zone and habitat on the speciation rates.
232
233 Finally, to test the effect of dispersal capacity, we assessed the relationship between
234 spore size and speciation rate for the few (n=32) VT that contain sequences of
235 morphologically characterized AMF isolates [57]. We gathered measures of their average
236 spore length [57] and tested their relationship with speciation rate by using a phylogenetic
237 generalized least square regression (PGLS).
238
239 **Estimating genetic diversity:**
240
241 As a first attempt at connecting AMF macroevolutionary diversification to
242 microevolutionary processes, we measured intraspecific genetic diversities across AMF
243 units. For each AMF unit containing at least 10 sequences, we computed genetic diversity
244 using Tajima's estimator [58]($\theta\pi$; Supplementary Methods 6). Using similar statistical tests
245 as above, we investigated the correlation of AMF genetic diversity with speciation rate,
246 niche width, geographic characteristics, and spore size. We tested the robustness of the
247 results to the minimal number of sequences per AMF unit (10, 15 or 20) used to compute
248 genetic diversity and to perform the PCA.
249

250 These statistical models were replicated on the different phylogenetic trees
251 (consensus or replicates) for each delineation and we reported p-values (*P*) corresponding
252 to two-sided tests.
253

Results:

AMF species delineations & phylogenetic reconstructions:

The EU97.5 and EU98 delineations (obtained using a threshold of 97.5% and 98% respectively) provided a number of AMF units (340 and 641) comparable to the 384 currently recognized VT, while the EU97 delineation had much less (182). Conversely, the EU98.5 and EU99 delineations yielded a much larger number of AMF units (1,190 and 2,647, respectively; Supplementary Tables 3 & 4) that was consistent with the number obtained using GMYC analyses (Supplementary Tables 4 & 5). This supports the idea that some VT might lump together several cryptic species [16](Supplementary Note 1), and that a 98.5 or 99% similarity threshold is more relevant for AMF species delineation. In addition, the GMYC indicated that the actual level of genetic variation within the SSU marker is overall sufficient to separate AMF species-like units among SSU haplotypes (GMYC LRT: $P<0.05$; Supplementary Fig. 2); on average, there are 10 SSU haplotypes for one AMF unit delineated using GMYC (Supplementary Table 5). Rarefaction curves as well as Bayesian and Chao2 estimates of diversity suggested that more than 90% of the total diversity of AMF is represented in our dataset regardless of the delineation threshold (Fig. 1b, Supplementary Tables 2, 5, & 6; Supplementary Note 2), which is consistent with the proportion of new AMF units detected in recent studies [59].

The reconstructed Bayesian phylogenetic trees based on VT and EU species delineations did not yield high support for the nodes separating the main AMF orders; yet, they had similar topologies and branching times of the internal nodes overall (Fig. 2, Supplementary Figs. 3). As expected, finer delineations resulted in an increase in the number of nodes close to the present (Supplementary Figs. 4). However, we observed a slowdown in the accumulation of new lineages close to the present in all lineage through time plots (LTTs), including those with the finest delineations (EU98.5 and EU99; Supplementary Fig. 5).

Temporal diversification dynamics:

AMF speciation rates ranged from 0.005 to 0.03 events per lineage per Myr (Fig. 2; Supplementary Fig. 6), and varied both within and among AMF orders, with Glomerales and Diversisporales having the highest present-day speciation rates (Supplementary Fig. 7). AMF experienced their most rapid diversification between 200 and 100 Myr ago according to estimates of diversification rates through time obtained with ClaDS (Fig. 2; Supplementary Fig. 8), and 150-50 Myr ago according to diversification models with piecewise constant rates (TreePar [48] and CoMET [50], Fig. 2; Supplementary Figs. 9 & 10).

The fast diversification of AMF around 150 Myr ago was followed by a slowdown in the recent past (Fig. 2; Supplementary Fig. 8), as suggested by the plateauing of the LTTs. A global decrease of the speciation rates through time was independently supported by ClaDS, TreePar, and CoMET analyses (Supplementary Figs. 11, 9 & 10), as well as time-dependent models in RPANDA [60](Supplementary Fig. 12). This slowdown was robust to all species delineations (Supplementary Figs. 8, 9, 10, & 12), the branching process prior (analyses not shown), phylogenetic uncertainty, and sampling fractions down to 50%, except in ClaDS analyses where the trend disappeared in some EU99 trees and for sampling fractions lower than 70% (Supplementary Figs. 13, 14, & 15).

We did not find a strong signal of extinction in our analyses: the turnover rate estimated from ClaDS was generally close to zero (Supplementary Fig. 11b), and models including extinctions were never selected in RPANDA (Supplementary Fig. 12). Similarly, the extinction rates estimated in piecewise-constant models were not significantly different from 0 (Supplementary Fig. 16).

312 **AMF diversification drivers:**

313

314 When fitting environment-dependent models of diversification, we found high
315 support for temperature-dependent models compared to time-dependent models for all
316 AMF delineations, sampling fractions, and crown ages (Fig. 3; Supplementary Figs. 17, 18,
317 19, 20, & 21), with the exception of some EU99 trees with a 50% sampling fraction
318 (Supplementary Fig. 21). This signal of temperature dependency was not due to a temporal
319 trend (Supplementary Note 3) nor to an artefact caused by rate heterogeneities
320 (Supplementary Note 4). Evidence for temperature dependency, however, decreased in
321 some clades closer to the present (see Methods), as small trees tend to be best fit by constant
322 rather than environment-dependent models (Supplementary Fig. 22). We detected a
323 significant positive dependency of the diversification rates on CO_2 concentrations in some
324 sub-trees, but rarely found a significant effect of plant fossil diversity (Supplementary Fig.
325 22).

326

327 The PCA of AMF niche width characteristics had a first principal component (PC1)
328 that indicated the propensity of each AMF unit (VT or EUs) to be vastly distributed among
329 continents, ecosystems and/or associated with many plant species and lineages, whereas
330 the second principal component (PC2) indicated the propensity of a given AMF unit to
331 associate with few plant species on many continents (Fig. 4; Supplementary Fig. 23 & 24).
332 Hence, PC1 reflects AMF niche width, whereas PC2 discriminates the width of the abiotic
333 relatively to the biotic niche (Fig. 4a-b; Supplementary Fig. 25). We found a positive
334 correlation between PC1 and lineage-specific speciation rates in the majority of the VT and
335 EU99 trees (Fig. 4c-d; Supplementary Fig. 26a). However, these results were no longer
336 significant when controlling for phylogenetic non-independence between AMF units
337 (Supplementary Fig. 26b), likely because a single *Glomeraceae* clade, including the abundant
338 and widespread morphospecies *Rhizophagus irregularis* and *R. clarus,* had both the highest
339 speciation rates among AMF (Fig. 2a-b) and the largest niche widths (Supplementary Fig.
340 27).

We found no effect of latitude on speciation rates, regardless of the AMF delineation or the minimum number of sequences per AMF unit (MCMCglmm: $P>0.05$), and no effect of habitat or climatic zone either (Supplementary Fig. 28). Similarly, we recovered no significant correlation between spore size and speciation rate (Supplementary Fig. 29), nor between spore size and level of endemism (Supplementary Fig. 30).

Finally, Tajima's $\theta\pi$ estimator of AMF genetic diversity was significantly and positively correlated with niche width (PC1) for all AMF delineations and minimal number of sequences per AMF unit considered, and in particular with abiotic aspects of the niche (PC2) in many cases (Fig. 4e-h; Supplementary Fig. 26). Genetic diversity was not correlated with speciation rate (Supplementary Fig. 26), latitude, habitat, climatic zone (MCMCglmm: $P>0.05$), or spore size (PGLS: $P>0.05$).

354 *Discussion*

355

356 **AMF species delineations, diversity, and phylogeny:**

357

358 The species concept is difficult to apply in AMF, which are poorly differentiated
359 morphologically and mainly characterized by environmental sequences [16]. In addition,
360 their reproduction mode is not well known and they have unique nuclear dynamics in
361 their spores and hyphae [61]. Our GMYC analyses suggest that biologically relevant AMF
362 species-like units correspond to SSU rRNA haplotypes with a sequence similarity between
363 98.5 and 99%. With this criterion of species delineation, we estimate that there are between
364 1,300 and 2,900 AMF 'species'. These estimates are largely above the number of currently
365 described morphospecies or VT (Supplementary Note 1) but remain low in comparison
366 with other fungal groups, like the Agaricomycetes that include taxa forming
367 ectomycorrhiza [62].

368

369 Species delineations and phylogenies constructed from a single gene and short
370 sequences are limited, but in the current state of data acquisition, relatively short
371 metabarcoding sequences provide for most microbial groups, including AMF, the only
372 current possibility to analyze their diversification dynamics [20, 63, 64]. Here, our
373 phylogenies did not resolve the branching of the AMF orders, with node supports similar
374 to those of previous studies [12, 17, 20](Supplementary Note 5), confirming that additional
375 genomic evidence is required to reach consensus. We considered this uncertainty in the
376 phylogenetic reconstruction by repeating our analyses on a set of trees spanning the likely
377 tree space. We hope that our study based on the SSU rRNA region alone will foster efforts
378 to obtain more genetic data, including additional genes and genomic information, with the
379 aim of reconstructing better supported, comprehensive phylogenies.

380

381

382

383 **AMF diversify slowly:**

384

385 We found speciation rates for AMF an order of magnitude lower than rates typically
386 found for macro-eukaryotes [46, 65], like plants [29], or Agaricomycetes [62]. Low
387 speciation rates in AMF may be linked to their (debated) asexual reproduction [66], to their
388 occasional long-distance dispersal that homogenizes populations globally over
389 evolutionary timescales [67], or to the fact that they are generalist obligate symbionts [68].
390 Regardless of the proximal cause, and contrary to Agaricomycetes for example, which
391 present a large diversity of species, morphologies, and ecologies, the niche space exploited
392 by AMF is limited to plant roots and the surrounding soil because of their obligate
393 dependence on plants for more than 400 Myr [69, 70]. Thus, although AMF species
394 delineation based on the SSU rRNA gene can be a poor predictor of their functional
395 diversity, our analyses based on this gene has revealed that AMF, despite their ubiquity,
396 have poorly diversified in the last 500 Myr compared with other groups.

397

398 We found little evidence for species extinction in AMF, including at mass extinction
399 events. Although AMF are relatively widespread and generalists, and low extinction rates
400 have been predicted before based on their ecology [2], these low extinction rate estimates
401 could also come from the difficulty of estimating extinction from molecular phylogenies
402 [71], one of the limitations of phylogeny-based diversification analyses (Supplementary
403 Note 6).

404

405 **AMF diversification through time:**

406

407 The observed peak of AMF diversification detected between 200 and 100 Myr (or 150-
408 50 Myr according to the models) was mainly linked to the fast diversification of the largest
409 family Glomeraceae (Fig. 2). This peak was concomitant with the radiation of flowering
410 plants [28], but also with a major continental reconfiguration, including the breakdown of
411 Pangea and the formation of climatically contrasted landmasses [20]. This period was also

412 characterized by a warm climate potentially favorable to AMF diversification, such that
413 disentangling the impact of these various factors on AMF diversification is not
414 straightforward. Interestingly, a peak of diversification at this period was also found in the
415 Agaricomycetes forming ectomycorrhiza [62].
416
417 This peak of diversification has been followed by a slowdown. Signals of
418 diversification slowdowns sometimes result from methodological artifacts, including
419 incorrect species delineations or under-sampling [72]. We carefully considered uncertainty
420 in species delineations and under-sampling down to 50%. In addition, our GMYC analyses
421 confirmed that the SSU rRNA gene evolves fast enough to delineate AMF species-like
422 units; although some cryptic AMF species can have the same SSU sequence [12], our
423 analyses support the overall existence of several SSU haplotypes per AMF unit.
424 Slowdowns in diversification rates close to the present have often been interpreted as a
425 progressive reduction of the number of available niches as species diversify and
426 accumulate [72, 73]. In AMF, this potential effect of niche saturation could be exacerbated
427 by a reduction of their niches linked to both repetitive breakdowns of their symbiosis with
428 plants and climatic changes. Indeed, in the last 100 Myr, many plant lineages evolved
429 alternative root symbioses or became non-symbiotic [5, 32, 33, 74]: approximately 20% of
430 extant plants do not interact with AMF anymore [4]. Additionally, the cooling of the Earth
431 during the Cenozoic reduced the surface of tropical regions [75, 76], which tend to be a
432 reservoir of ecological niches for AMF [20, 32, 77].
433
434 The difficulty of reconstructing past symbiotic associations prevents direct testing of
435 the hypothesis that the emergence of new root symbioses in plants led to a diversification
436 slowdown in AMF. However, we tested the hypothesis that global temperature changes
437 affected diversification rates and found a strong relationship (Fig. 3). Such associations
438 between temperature and diversification rates have been observed before in eukaryotes
439 and have several potential causes [78]. Two prevailing hypotheses are the evolutionary
440 speed hypothesis, stipulating that high temperatures entail higher mutation rates and

441 faster speciation [79], and the productivity hypothesis, stating that resources and
442 associated ecological niches are more numerous in warm and productive environments,
443 especially when the tropics are large [80]. The latter hypothesis is particularly relevant for
444 AMF, which have many host plant niches in the tropics and potentially less in temperate
445 regions [81], where a higher proportion of plants are non-mycorrhizal [82] or
446 ectomycorrhizal [32, 62]. Hence, the observed effect of past global temperatures could
447 reflect the shrinkage of tropical areas and the associated decrease of the relative proportion
448 of arbuscular mycorrhizal plants.
449
450 A few AMF clades displayed a significant support for diversification models with a
451 positive dependency on CO_2 concentrations, which reinforces the idea that for the
452 corresponding AMF, benefits retrieved from plants could have been amplified by high CO_2
453 concentrations and fostered diversification [83, 84]. Conversely, we found a limited effect
454 of land plant fossil diversity, which indicates that variations in the tempo of AMF
455 diversification did not systematically follow those of land plants. Still, the possible
456 concordance of the peak of AMF diversification with the radiation of the Angiosperms is
457 noteworthy, in particular in Glomeraceae that frequently interact with present-day
458 Angiosperms [17]. The co-diversification with the plants might have been an important
459 driver from the emergence of land plants until the Mesozoic [2, 10], but less so thereafter,
460 when AMF diversification declined while some flowering plants radiated, including AMF-
461 free groups such as the species-rich Orchidaceae, blurring co-diversification patterns
462 (Supplementary Fig. 31)[30, 85].
463
464 **AMF recent diversification:**
465
466 Looking at the correlates of AMF present-day diversification rates, we found no effect
467 of habitat or climatic zone, even though AMF are more frequent and diverse in the tropics
468 (Supplementary Fig. 32)[20, 25, 81] and their speciation rates are positively correlated with
469 global temperature. Further work, including a more thorough sampling of the distribution

470 of AMF species across latitudes and habitats, would be required to confirm these patterns
471 and to distinguish whether speciation events are indeed no more frequent in the tropics or,
472 if they are, whether long-distance dispersal redistributes the new lineages at different
473 latitudes over evolutionary time scales [25]. Similarly, although the temporal changes in
474 the availability of AMF niches likely influenced the diversification of the group, we found
475 little support for AMF species with larger niche width having higher lineage-specific
476 speciation rates (Fig. 4). We also note that there are important aspects of the niche that we
477 do not (and yet cannot) account for in our characterization of AMF niche width: it is
478 thought that some AMF species may mainly provide mineral nutrients extracted from the
479 soil, whereas others may be more specialized in protecting plants from biotic or abiotic
480 stresses [86] and such (inter- or intra-specific) functional variations may have evolutionary
481 significance. Finally, although spore size is often inversely related to dispersal capacity
482 [87], which can either promote diversification by favoring founder speciation events, or
483 limit diversification by increasing gene flow, we found no significant correlation between
484 spore size and diversification rates, which may be explained either by a weak or absent
485 effect or by the low number of species for which this data is available. In addition, the
486 absence of correlation between spore size and level of endemism suggests that even AMF
487 with large spores experience long-distance dispersal [57, 88]. Thus, if large spores might
488 limit dispersal at smaller (e.g. intra-continental) scales in AMF [22, 89], this does not seem
489 to affect diversification.
490
491 In AMF, intraspecific variability is an important source of functional diversity [67,
492 90] and their genetic diversity may indicate the intraspecific variability on which selection
493 can act, potentially leading to species diversification. Here, geographically widespread
494 AMF species appear to be more genetically diverse, as previously suggested by population
495 genomics [67], but do not necessarily speciate faster. Along with a decoupling between
496 genetic diversity and lineage-specific speciation rate, this suggests that the accumulation
497 of genetic diversity among distant subpopulations is not enough to spur AMF speciation.
498

499 **Conclusion:**

500

501 Our findings that AMF have low speciation rates, likely constrained by the
502 availability of suitable niches, reinforce the vision of AMF as an "evolutionary cul-de-sac"
503 [1]. We interpret the significant diversification slowdown in the past 100 Myr as the
504 conjunction of the emergence of plant lineages not associated with AMF and the reduction
505 of tropical areas induced by climate cooling, in the context of obligate dependence of AMF
506 on plants. Diversification slowdowns have often been interpreted as the signal of adaptive
507 radiations [72, 91], that is clades that experienced a rapid accumulation of morphological,
508 ecological, and species diversity [92]. AMF provide a striking example of a clade with slow
509 morphological, ecological and species diversification that features a pattern of
510 diversification slowdown. In AMF, and potentially in many other species groups [78], such
511 a slowdown likely reflects a reduction of the global availability of ecological niches.

512 **References:**

513

514 1. Malloch DM. The evolution of mycorrhizae. *Can J Plant Path* 1987; **9**: 398–402.

515 2. Morton JB. Species and clones of arbuscular mycorrhizal fungi (Glomales,
516 Zygomycetes): their role in macro- and microevolutionary processes. *Mycotaxon*
517 *(USA)* 1990; **37**: 493–515.

518 3. Smith SE, Read DJ. Mycorrhizal Symbiosis. *Mycorrhizal Symbiosis* . 2008. Elsevier.

519 4. van der Heijden MGAA, Martin FM, Selosse M-A, Sanders IR. Mycorrhizal ecology
520 and evolution: the past, the present, and the future. *New Phytol* 2015; **205**: 1406–
521 1423.

522 5. Selosse M-A, Le Tacon F. The land flora: a phototroph-fungus partnership? *Trends*
523 *Ecol Evol* 1998; **13**: 15–20.

524 6. Field KJ, Pressel S, Duckett JG, Rimington WR, Bidartondo MI. Symbiotic options
525 for the conquest of land. *Trends Ecol Evol* 2015; **30**: 477–486.

526 7. Feijen FAA, Vos RA, Nuytinck J, Merckx VSFT. Evolutionary dynamics of
527 mycorrhizal symbiosis in land plant diversification. *Sci Rep* 2018; **8**: 10698.

528 8. Strullu-Derrien C, Selosse MA, Kenrick P, Martin FM. The origin and evolution of
529 mycorrhizal symbioses: from palaeomycology to phylogenomics. *New Phytol* 2018;
530 **220**: 1012–1030.

531 9. Simon L, Bousquet J, Lévesque RC, Lalonde M. Origin and diversification of
532 endomycorrhizal fungi and coincidence with vascular land plants. *Nature* 1993; **363**:
533 67–69.

534 10. Lutzoni F, Nowak MD, Alfaro ME, Reeb V, Miadlikowska J, Krug M, et al.
535 Contemporaneous radiations of fungi and plants linked to symbiosis. *Nat Commun*
536 2018; **9**: 1–11.

537 11. Stürmer SL. A history of the taxonomy and systematics of arbuscular mycorrhizal
538 fungi belonging to the phylum Glomeromycota. *Mycorrhiza* 2012; **22**: 247–258.

539 12. Krüger M, Krüger C, Walker C, Stockinger H, Schüßler A. Phylogenetic reference
540 data for systematics and phylotaxonomy of arbuscular mycorrhizal fungi from

541 phylum to species level. *New Phytol* 2012; **193**: 970–984.
542 13. Öpik M, Vanatoa A, Vanatoa E, Moora M, Davison J, Kalwij JM, et al. The online
543 database MaarjAM reveals global and ecosystemic distribution patterns in
544 arbuscular mycorrhizal fungi (Glomeromycota). *New Phytol* 2010; **188**: 223–241.
545 14. Öpik M, Davison J, Moora M, Zobel M. DNA-based detection and identification of
546 Glomeromycota: the virtual taxonomy of environmental sequences. *Botany* 2014; **92**:
547 135–147.
548 15. Powell JR, Monaghan MT, Öpik M, Rillig MC. Evolutionary criteria outperform
549 operational approaches in producing ecologically relevant fungal species
550 inventories. *Mol Ecol* 2011; **20**: 655–666.
551 16. Bruns TD, Corradi N, Redecker D, Taylor JW, Öpik M. Glomeromycotina: what is a
552 species and why should we care? *New Phytol* 2018; **220**: 963–967.
553 17. Rimington WR, Pressel S, Duckett JG, Field KJ, Read DJ, Bidartondo MI. Ancient
554 plants with ancient fungi: liverworts associate with early-diverging arbuscular
555 mycorrhizal fungi. *Proc R Soc B Biol Sci* 2018; **285**: 20181600.
556 18. James TY, Kauff F, Schoch CL, Matheny PB, Hofstetter V, Cox CJ, et al.
557 Reconstructing the early evolution of Fungi using a six-gene phylogeny. *Nature*
558 2006; **443**: 818–822.
559 19. Venice F, Ghignone S, Salvioli di Fossalunga A, Amselem J, Novero M, Xianan X, et
560 al. At the nexus of three kingdoms: the genome of the mycorrhizal fungus
561 Gigaspora margarita provides insights into plant, endobacterial and fungal
562 interactions. *Environ Microbiol* 2020; **22**: 122–141.
563 20. Davison J, Moora M, Opik M, Adholeya A, Ainsaar L, Ba A, et al. Global
564 assessment of arbuscular mycorrhizal fungus diversity reveals very low endemism.
565 *Science (80-)* 2015; **349**: 970–973.
566 21. Egan C, Li D-W, Klironomos J. Detection of arbuscular mycorrhizal fungal spores
567 in the air across different biomes and ecoregions. *Fungal Ecol* 2014; **12**: 26–31.
568 22. Bueno CG, Moora M. How do arbuscular mycorrhizal fungi travel? *New Phytol*
569 2019; **222**: 645–647.

570 23. Correia M, Heleno R, da Silva LP, Costa JM, Rodríguez-Echeverría S. First evidence
571 for the joint dispersal of mycorrhizal fungi and plant diaspores by birds. *New Phytol*
572 2019; **222**: 1054–1060.
573 24. Templeton AR. The reality and importance of founder speciation in evolution.
574 *BioEssays* . 2008. John Wiley & Sons, Ltd. , **30**: 470–479
575 25. Pärtel M, Öpik M, Moora M, Tedersoo L, Szava-Kovats R, Rosendahl S, et al.
576 Historical biome distribution and recent human disturbance shape the diversity of
577 arbuscular mycorrhizal fungi. *New Phytol* 2017; **216**: 227–238.
578 26. Perez-Lamarque B, Selosse M, Öpik M, Morlon H, Martos F. Cheating in arbuscular
579 mycorrhizal mutualism: a network and phylogenetic analysis of
580 mycoheterotrophy. *New Phytol* 2020; **226**: 1822–1835.
581 27. Sanders IR. Preference, specificity and cheating in the arbuscular mycorrhizal
582 symbiosis. *Trends Plant Sci* 2003; **8**: 143–145.
583 28. Sauquet H, Magallón S. Key questions and challenges in angiosperm
584 macroevolution. *New Phytol* 2018; **219**: 1170–1187.
585 29. Zanne AE, Tank DC, Cornwell WK, Eastman JM, Smith SA, FitzJohn RG, et al.
586 Three keys to the radiation of angiosperms into freezing environments. *Nature*
587 2014; **506**: 89–92.
588 30. Cleal CJ, Cascales-Miñana B. Composition and dynamics of the great Phanerozoic
589 Evolutionary Floras. *Lethaia* 2014; **47**: 469–484.
590 31. Bredenkamp GJ, Spada F, Kazmierczak E. On the origin of northern and southern
591 hemisphere grasslands. *Plant Ecol* 2002; **163**: 209–229.
592 32. Brundrett MC, Tedersoo L. Evolutionary history of mycorrhizal symbioses and
593 global host plant diversity. *New Phytol* 2018; **220**: 1108–1115.
594 33. Werner GDA, Cornelissen JHC, Cornwell WK, Soudzilovskaia NA, Kattge J, West
595 SA, et al. Symbiont switching and alternative resource acquisition strategies drive
596 mutualism breakdown. *Proc Natl Acad Sci* 2018; **115**: 5229–5234.
597 34. Werner GDA, Cornwell WK, Sprent JI, Kattge J, Kiers ET. A single evolutionary
598 innovation drives the deep evolution of symbiotic N2-fixation in angiosperms. *Nat*

599 *Commun* 2014; **5**: 4087.
600 35. Lekberg Y, Vasar M, Bullington LS, Sepp S-K, Antunes PM, Bunn R, et al. More
601 bang for the buck? Can arbuscular mycorrhizal fungal communities be
602 characterized adequately alongside other fungi using general fungal primers? *New*
603 *Phytol* 2018; **220**: 971–976.
604 36. Katoh K, Standley DM. MAFFT Multiple sequence alignment software version 7:
605 Improvements in performance and usability. *Mol Biol Evol* 2013; **30**: 772–780.
606 37. Bouckaert R, Heled J, Kühnert D, Vaughan T, Wu C-H, Xie D, et al. BEAST 2: a
607 software platform for Bayesian evolutionary analysis. *PLoS Comput Biol* 2014; **10**:
608 e1003537.
609 38. Simon L, Lalonde M, Bruns TD. Specific amplification of 18S fungal ribosomal
610 genes from vesicular-arbuscular endomycorrhizal fungi colonizing roots. *Appl*
611 *Environ Microbiol* 1992; **58**: 291–5.
612 39. Lee J, Lee S, Young JPW. Improved PCR primers for the detection and
613 identification of arbuscular mycorrhizal fungi. *FEMS Microbiol Ecol* 2008; **65**: 339–
614 349.
615 40. Morlon H, Lewitus E, Condamine FL, Manceau M, Clavel J, Drury J. RPANDA: An
616 R package for macroevolutionary analyses on phylogenetic trees. *Methods Ecol Evol*
617 2016; **7**: 589–597.
618 41. R Core Team. R: A language and environment for statistical computing. 2019. R
619 Foundation for Statistical Computing, Vienna, Austria.
620 42. Fujisawa T, Barraclough TG. Delimiting species using single-locus data and the
621 generalized mixed yule coalescent approach: A revised method and evaluation on
622 simulated data sets. *Syst Biol* 2013; **62**: 707–724.
623 43. Pons J, Barraclough TG, Gomez-Zurita J, Cardoso A, Duran DP, Hazell S, et al.
624 Sequence-based species delimitation for the DNA taxonomy of undescribed insects.
625 *Syst Biol* 2006; **55**: 595–609.
626 44. Ezard T, Fujisawa T, Barraclough TG. SPLITS: SPecies' LImits by Threshold
627 Statistics. 2009. , R package

45. Quince C, Curtis TP, Sloan WT. The rational exploration of microbial diversity. *ISME J* 2008; **2**: 997–1006.
46. Maliet O, Hartig F, Morlon H. A model with many small shifts for estimating species-specific diversification rates. *Nat Ecol Evol* 2019; **3**: 1086–1092.
47. Gelman A, Rubin DB. Inference from iterative simulation using multiple sequences. *Stat Sci* 1992; **7**: 457–472.
48. Stadler T. Mammalian phylogeny reveals recent diversification rate shifts. *Proc Natl Acad Sci* 2011; **108**: 6187–6192.
49. Höhna S, May MR, Moore BR. TESS: An R package for efficiently simulating phylogenetic trees and performing Bayesian inference of lineage diversification rates. *Bioinformatics* 2016; **32**: 789–791.
50. May MR, Höhna S, Moore BR. A Bayesian approach for detecting the impact of mass-extinction events on molecular phylogenies when rates of lineage diversification may vary. *Methods Ecol Evol* 2016; **7**: 947–959.
51. Condamine FL, Rolland J, Morlon H. Macroevolutionary perspectives to environmental change. *Ecol Lett* 2013; **16**: 72–85.
52. Rabosky DL, Lovette IJ. Density-dependent diversification in North American wood warblers. *Proc R Soc B Biol Sci* 2008; **275**: 2363–2371.
53. Royer DL, Berner RA, Montanez IP, Tabor NJ, Beerling DJ. CO2 as a primary driver of Phanerozoic climate. *GSA Today* 2004; **14**: 4–10.
54. Foster GL, Royer DL, Lunt DJ. Future climate forcing potentially without precedent in the last 420 million years. *Nat Commun* 2017; **8**: 14845.
55. Alroy J. Geographical, environmental and intrinsic biotic controls on Phanerozoic marine diversification. *Palaeontology* 2010; **53**: 1211–1235.
56. Hadfield JD. MCMC methods for multi-response generalized linear mixed models: The MCMCglmm R package. *J Stat Softw* 2010; **33**: 1–22.
57. Davison J, Moora M, Öpik M, Ainsaar L, Ducousso M, Hiiesalu I, et al. Microbial island biogeography: isolation shapes the life history characteristics but not diversity of root-symbiotic fungal communities. *ISME J* 2018; **12**: 2211–2224.

657 58. Tajima F. Evolutionary relationship of DNA sequences in finite populations.
658 *Genetics* 1983; **105**: 437–460.
659 59. Sepp S, Davison J, Jairus T, Vasar M, Moora M, Zobel M, et al. Non-random
660 association patterns in a plant–mycorrhizal fungal network reveal host–symbiont
661 specificity. *Mol Ecol* 2019; **28**: 365–378.
662 60. Morlon H, Parsons TL, Plotkin JB. Reconciling molecular phylogenies with the
663 fossil record. *Proc Natl Acad Sci* 2011; **108**: 16327–16332.
664 61. Kokkoris V, Stefani F, Dalpé Y, Dettman J, Corradi N. Nuclear dynamics in the
665 arbuscular mycorrhizal fungi. *Trends Plant Sci* 2020; **25**: 765–778.
666 62. Varga T, Krizsán K, Földi C, Dima B, Sánchez-García M, Sánchez-Ramírez S, et al.
667 Megaphylogeny resolves global patterns of mushroom evolution. *Nat Ecol Evol*
668 2019; **3**: 668–678.
669 63. Louca S, Shih PM, Pennell MW, Fischer WW, Parfrey LW, Doebeli M. Bacterial
670 diversification through geological time. *Nat Ecol Evol* 2018; **2**: 1458–1467.
671 64. Lewitus E, Bittner L, Malviya S, Bowler C, Morlon H. Clade-specific diversification
672 dynamics of marine diatoms since the Jurassic. *Nat Ecol Evol* 2018; **2**: 1715–1723.
673 65. Upham NS, Esselstyn JA, Jetz W. Inferring the mammal tree: Species-level sets of
674 phylogenies for questions in ecology, evolution, and conservation. *PLoS Biol* 2019;
675 **17**: e3000494.
676 66. Yildirir G, Malar C M, Kokkoris V, Corradi N. Parasexual and sexual reproduction
677 in arbuscular mycorrhizal fungi: Room for both. *Trends Microbiol* 2020; **28**: 517–519.
678 67. Savary R, Masclaux FG, Wyss T, Droh G, Cruz Corella J, Machado AP, et al. A
679 population genomics approach shows widespread geographical distribution of
680 cryptic genomic forms of the symbiotic fungus Rhizophagus irregularis. *ISME J*
681 2018; **12**: 17–30.
682 68. Morlon H, Kemps BD, Plotkin JB, Brisson D. Explosive radiation of a bacterial
683 species group. *Evolution (N Y)* 2012; **66**: 2577–2586.
684 69. Tisserant E, Malbreil M, Kuo A, Kohler A, Symeonidi A, Balestrini R, et al. Genome
685 of an arbuscular mycorrhizal fungus provides insight into the oldest plant

686 symbiosis. *Proc Natl Acad Sci U S A* 2013; **110**: 20117–22.
687 70. Rich MK, Nouri E, Courty P-E, Reinhardt D. Diet of arbuscular mycorrhizal fungi:
688 Bread and butter? *Trends Plant Sci* 2017; **22**: 652–660.
689 71. Rabosky DL. Challenges in the estimation of extinction from molecular
690 phylogenies: A response to Beaulieu and O'Meara. *Evolution (N Y)* 2016; **70**: 218–
691 228.
692 72. Moen D, Morlon H. Why does diversification slow down? *Trends Ecol Evol* 2014; **29**:
693 190–197.
694 73. Rabosky DL. Ecological limits and diversification rate: Alternative paradigms to
695 explain the variation in species richness among clades and regions. *Ecol Lett* 2009;
696 **12**: 735–743.
697 74. Maherali H, Oberle B, Stevens PF, Cornwell WK, McGlinn DJ. Mutualism
698 persistence and abandonment during the evolution of the mycorrhizal symbiosis.
699 *Am Nat* 2016; **188**: E113–E125.
700 75. S. Meseguer A, Condamine FL. Ancient tropical extinctions at high latitudes
701 contributed to the latitudinal diversity gradient. *Evolution (N Y)* 2020; **74**: 1966–
702 1987.
703 76. Ziegler AM, Eshel G, McAllister Rees P, Rothfus TA, Rowley DB, Sunderlin D.
704 Tracing the tropics across land and sea: Permian to present. *Lethaia* 2003; **36**: 227–
705 254.
706 77. Read DJ. Mycorrhizas in ecosystems. *Experientia* 1991; **47**: 376–391.
707 78. Condamine FL, Rolland J, Morlon H. Assessing the causes of diversification
708 slowdowns: temperature-dependent and diversity-dependent models receive
709 equivalent support. *Ecol Lett* 2019; **22**: 1900–1912.
710 79. Rohde K. Latitudinal gradients in species diversity: The search for the primary
711 cause. *Oikos* 1992; **65**: 514.
712 80. Clarke A, Gaston KJ. Climate, energy and diversity. *Proc R Soc B Biol Sci* . 2006. The
713 Royal SocietyLondon. , **273**: 2257–2266
714 81. Toussaint A, Bueno G, Davison J, Moora M, Tedersoo L, Zobel M, et al.

Asymmetric patterns of global diversity among plants and mycorrhizal fungi. *J Veg Sci* 2020; **31**: 355–366.

82. Bueno CG, Moora M, Gerz M, Davison J, Öpik M, Pärtel M, et al. Plant mycorrhizal status, but not type, shifts with latitude and elevation in Europe. *Glob Ecol Biogeogr* 2017; **26**: 690–699.

83. Field KJ, Rimington WR, Bidartondo MI, Allinson KE, Beerling DJ, Cameron DD, et al. Functional analysis of liverworts in dual symbiosis with Glomeromycota and Mucoromycotina fungi under a simulated Palaeozoic CO2 decline. *ISME J* 2016; **10**: 1514–1526.

84. Humphreys CP, Franks PJ, Rees M, Bidartondo MI, Leake JR, Beerling DJ. Mutualistic mycorrhiza-like symbiosis in the most ancient group of land plants. *Nat Commun* 2010; **1**: 103.

85. Ramírez-Barahona S, Sauquet H, Magallón S. The delayed and geographically heterogeneous diversification of flowering plant families. *Nat Ecol Evol* 2020; **4**: 1232–1238.

86. Chagnon P-L, Bradley RL, Maherali H, Klironomos JN. A trait-based framework to understand life history of mycorrhizal fungi. *Trends Plant Sci* 2013; **18**: 484–491.

87. Nathan R, Schurr FM, Spiegel O, Steinitz O, Trakhtenbrot A, Tsoar A. Mechanisms of long-distance seed dispersal. *Trends Ecol Evol* 2008; **23**: 638–647.

88. Kivlin SN. Global mycorrhizal fungal range sizes vary within and among mycorrhizal guilds but are not correlated with dispersal traits. *J Biogeogr* 2020; **47**: 1994–2001.

89. Chaudhary VB, Nolimal S, Sosa-Hernández MA, Egan C, Kastens J. Trait-based aerial dispersal of arbuscular mycorrhizal fungi. *New Phytol* 2020; **228**: 238–252.

90. Munkvold L, Kjøller R, Vestberg M, Rosendahl S, Jakobsen I. High functional diversity within species of arbuscular mycorrhizal fungi. *New Phytol* 2004; **164**: 357–364.

91. Harmon LJ, Schulte JA, Larson A, Losos JB. Tempo and mode of evolutionary radiation in iguanian lizards. *Science (80-)* 2003; **301**: 961–964.

92. Simpson GG. The major features of evolution. 1953. Columbia University Press, New York.

93. Janzen T, Etienne RS. Inferring the role of habitat dynamics in driving diversification: evidence for a species pump in Lake Tanganyika cichlids. *bioRxiv* 2016; **11**: 1–18.

Acknowledgment:

The authors acknowledge C. Strullu-Derrien, M. Elias, D. de Vienne, A. Vogler, J.-Y. Dubuisson, C. Quince, S.-K. Sepp, and M. Chase for helpful discussions. They also thank L. Aristide, S. Lambert, J. Clavel, I. Quintero, I. Overcast, and G. Sommeria for comments on an early version of the manuscript and David Marsh for English editing. BPL acknowledges B. Robira, F. Foutel-Rodier, F. Duchenne, E. Faure, E. Kerdoncuff, R. Petrolli, and G. Collobert for useful discussions and C. Fruciano and E. Lewitus for providing codes. This work was supported by a doctoral fellowship from the École Normale Supérieure de Paris attributed to BPL and the École Doctorale FIRE – Programme Bettencourt. MÖ was supported by the European Regional Development Fund (Centre of Excellence EcolChange) and University of Tartu (PLTOM20903). Funding of the research of FM was from the Agence Nationale de la Recherche (ANR-19-CE02-0002). HM acknowledges support from the European Research Council (grant CoG-PANDA).

Author contributions:

All the authors designed the study. MÖ gathered the data and BPL performed the analyses. OM and ACAS provided some codes. BPL and HM wrote the first version of the manuscript and all authors contributed substantially to the revisions.

Competing Interests statement:

The authors declare that there is no conflict of interest.

Figures

Figure 1: Molecular-based species delineations of arbuscular mycorrhizal fungi (AMF) give consistent results and indicate a nearly complete sampling.

We compared the *virtual taxa* (VT) delineation from [13] with newly-developed automatic delineations into *evolutionary units* (EUs) based on an average threshold of similarity and a criterion of monophyly.

(a) The proportion of AMF units (VT or EUs) in each AMF family reveals constant proportions across delineations, although Glomeraceae tend to be relatively less numerous compared to the other AMF family in the VT delineation. The main AMF orders are indicated on the right of the charts: Paraglomerales + Archaeosporales, Diversisporales, and Glomerales (Glomeraceae + Claroideoglomeraceae).

(b) Rarefaction curves indicating the number of AMF units as a function of the percentage of sampled AMF accession revealed that the AMF sampling in MaarjAM is close to saturation for all delineations (VT or EUs). Rarefactions were performed 100 times every 5 percent and the median of the 100 replicates is represented here.

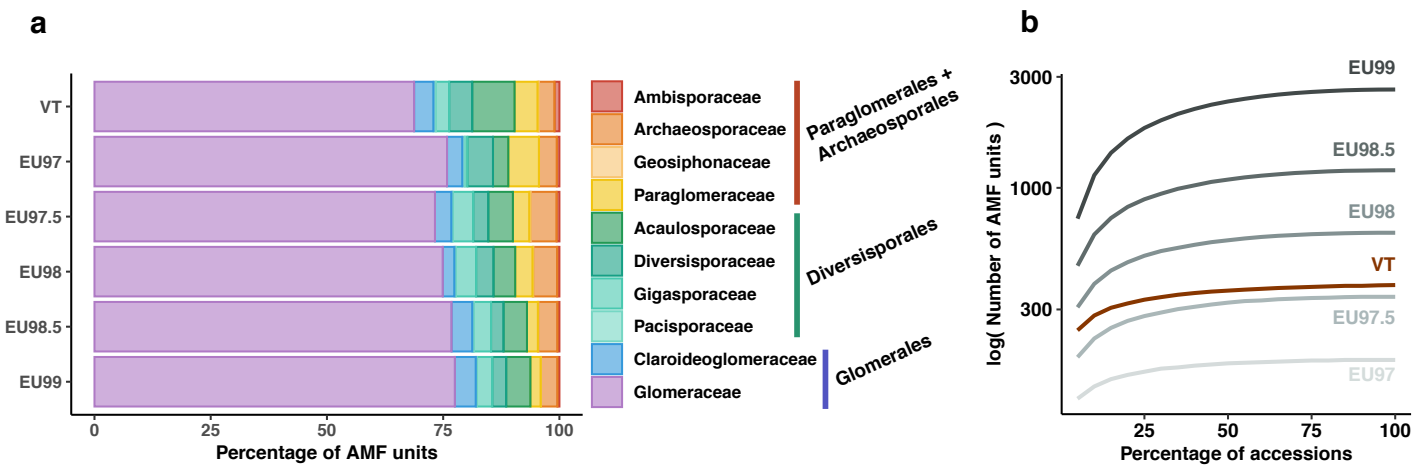

792 **Figure 2: The diversification dynamic of arbuscular mycorrhizal fungi (AMF) varies**
793 **significantly through time and between lineages.**
794
795 **(a-b):** AMF consensus phylogenetic trees corresponding to the VT (a) and EU99 (b) species
796 delineations. Branches are colored according to the lineage-specific speciation rates
797 estimated by ClaDS using the BDES estimated sampling fraction: lineages with low and
798 high speciation rates are represented in blue and red, respectively.
799 The main AMF clades are indicated with the following letters: *P* = Paraglomerales +
800 Archaeosporales, *D* = Diversisporales, *C* = Claroideoglomeraceae, and *G* = Glomeraceae.
801
802 **(c-d):** Mean speciation rates through time estimated by ClaDS, for the VT (c) and EU99 (d)
803 delineations and using the BDES estimated sampling fraction. The mean speciation rate
804 corresponds to the maximum *a posteriori* (MAP) of the mean speciation rate across all
805 fungal lineages back in time (including extinct and unsampled lineages). Orange and grey
806 lines represent the 12 independent replicate trees and the consensus tree, respectively.
807 Unlike most replicate trees, the EU99 consensus tree tends to present a limited
808 diversification slowdown, which reinforces the idea that consensus trees can be a
809 misleading representation [93].
810
811 **(e-f):** Net diversification rates (speciation rates minus extinction rates) through time
812 estimated by TreePar, for the VT (c) and EU99 (d) delineations and using the BDES
813 estimated sampling fraction. Orange and grey lines represent the 12 independent replicate
814 trees and the consensus tree, respectively.

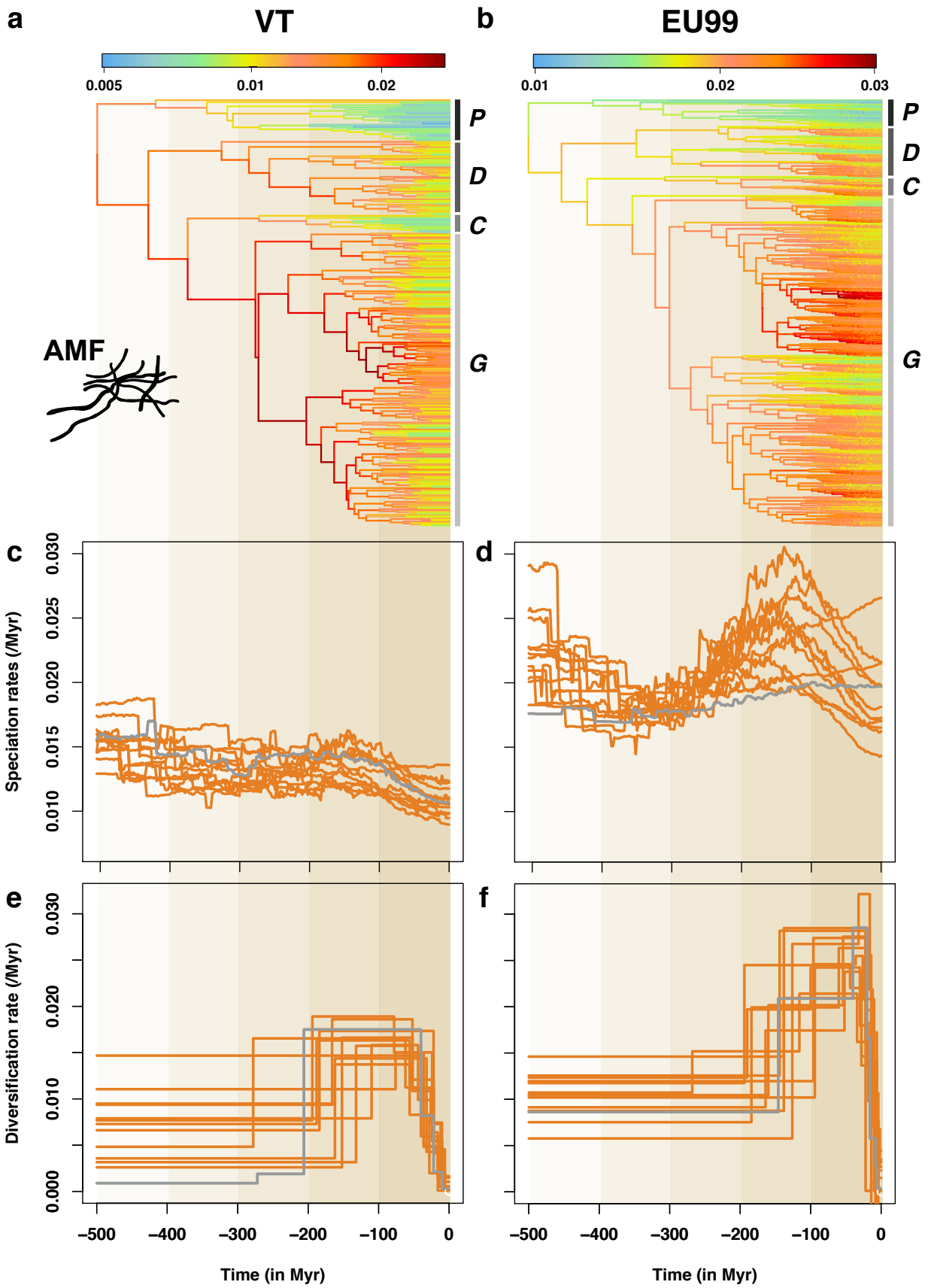
a
VT
b
EU99
0.005
0.01
0.02
0.01
0.02
0.03
P
D
C
G
AMF
c
d
e
f
Speciation rates (/Myr)
Diversification rate (/Myr)
0.010
0.015
0.020
0.025
0.030
0.000
−500
−400
−300
−200
−100
0
Time (in Myr)

815

816 **Figure 3: Temperature-dependent diversification models reveal that global temperature**
817 **positively associates with the speciation rates of arbuscular mycorrhizal fungi (AMF) in**
818 **the last 500 million years.**
819
820 **(a):** Average global temperature in the last 500 million years (Myr) relative to the average
821 temperature of the period 1960-1990. The smoothed orange line represents cubic splines
822 with 33 degrees of freedom used to fit temperature-dependent models of AMF
823 diversification with RPANDA. This default smoothing was estimated using the R function
824 *smooth.spline*.
825
826 **(b):** AICc difference between the best-supported time-dependent model and the
827 temperature-dependent model in RPANDA, for the VT (left) and EU99 (right) delineations,
828 using the BDES estimated sampling fraction. An AICc difference greater than 2 indicates
829 that there is significant support for the temperature-dependent model.
830
831 **(c):** Parameter estimations of the temperature-dependent models (speciation rate ~
832 exp(parameter * temperature)). A positive parameter value indicates a positive effect of
833 temperature on speciation rates.
834
835 For both delineations, the boxplots represent the results obtained for the consensus tree
836 and the 12 independent replicate trees. Boxplots indicate the median surrounded by the
837 first and third quartiles, and whiskers extend to the extreme values but no further than 1.5
838 of the inter-quartile range. The horizontal dotted lines highlighted the values estimated for
839 the consensus trees. Compared to the replicate trees, the consensus trees tend to present
840 extreme values (stronger support for temperature-dependent model), which reinforces the
841 idea that consensus trees can be a misleading representation [93].

842

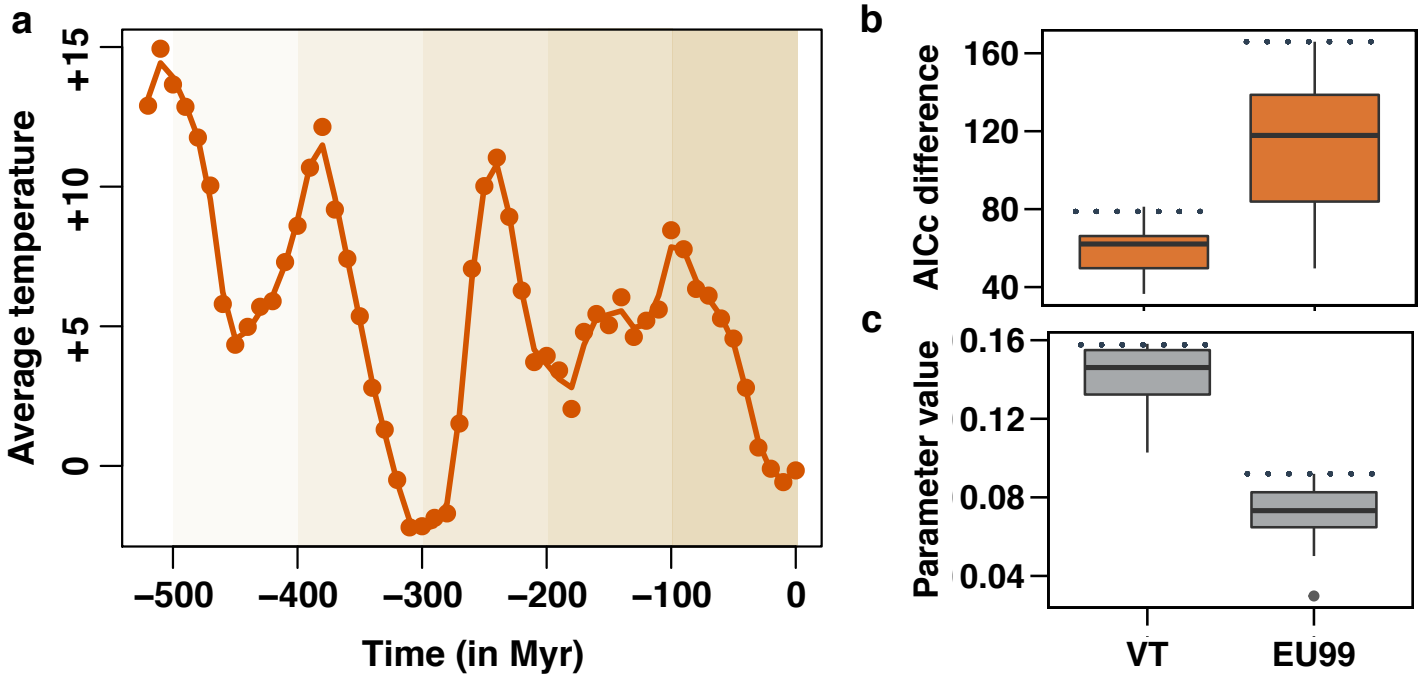
a
Average temperature
0
+5
+10
+15
−500
−400
−300
−200
−100
0
Time (in Myr)
b
AICc difference
160
120
80
40
c
Parameter value
0.16
0.12
0.08
0.04
VT
EU99

843 **Figure 4: Abiotic and biotic drivers of the species diversification and differentiation of**
844 **arbuscular mycorrhizal fungi (AMF)**
845 **(a-b):** Projection of 10 abiotic and biotic variables on the two principal coordinates
846 according to the VT (a) or EU99 (b) delineations. Principal coordinate analysis (PCA) was
847 performed for the AMF units represented by at least 10 sequences. Colors represent the
848 contribution of the variable to the principal coordinates. The percentage for each principal
849 coordinate (PC) indicates its amount of explained variance.
850 Tested variables were: the numbers of continents on which the AMF unit occurs
851 (nb_continent), of realms (nb_realm), of ecosystems (nb_ecosystems), of habitats
852 (nb_habitats), of biomes (nb_biomes), and climatic zones (nb_climatic) [13], as well as
853 information about the associated plant species of each unit, such as the number of plant
854 partners (nb_plants), the phylogenetic diversity of these plants (PD), and the betweenness
855 and closeness measurement of each fungal unit in the plant-fungus interaction network
856 (see Methods).
857
858 **(c-d):** Speciation rates as a function of the PC1 coordinates for each VT (c) or EU99 (d) unit.
859 Only the AMF consensus tree is represented here (other replicate trees are presented in
860 Supplementary Fig. 26).
861
862 **(e-h):** Genetic diversity (Tajima's $\theta\pi$ estimator) as a function of the PC1 (e-f) or PC2 (g-h)
863 coordinates for each VT (e-g) or EU99 (f-h) unit. Only the AMF consensus tree is
864 represented here (other replicate trees are presented in Supplementary Fig. 26). The grey
865 lines indicate the statistically significant linear regression between the two variables
866 inferred using MCMCglmm.

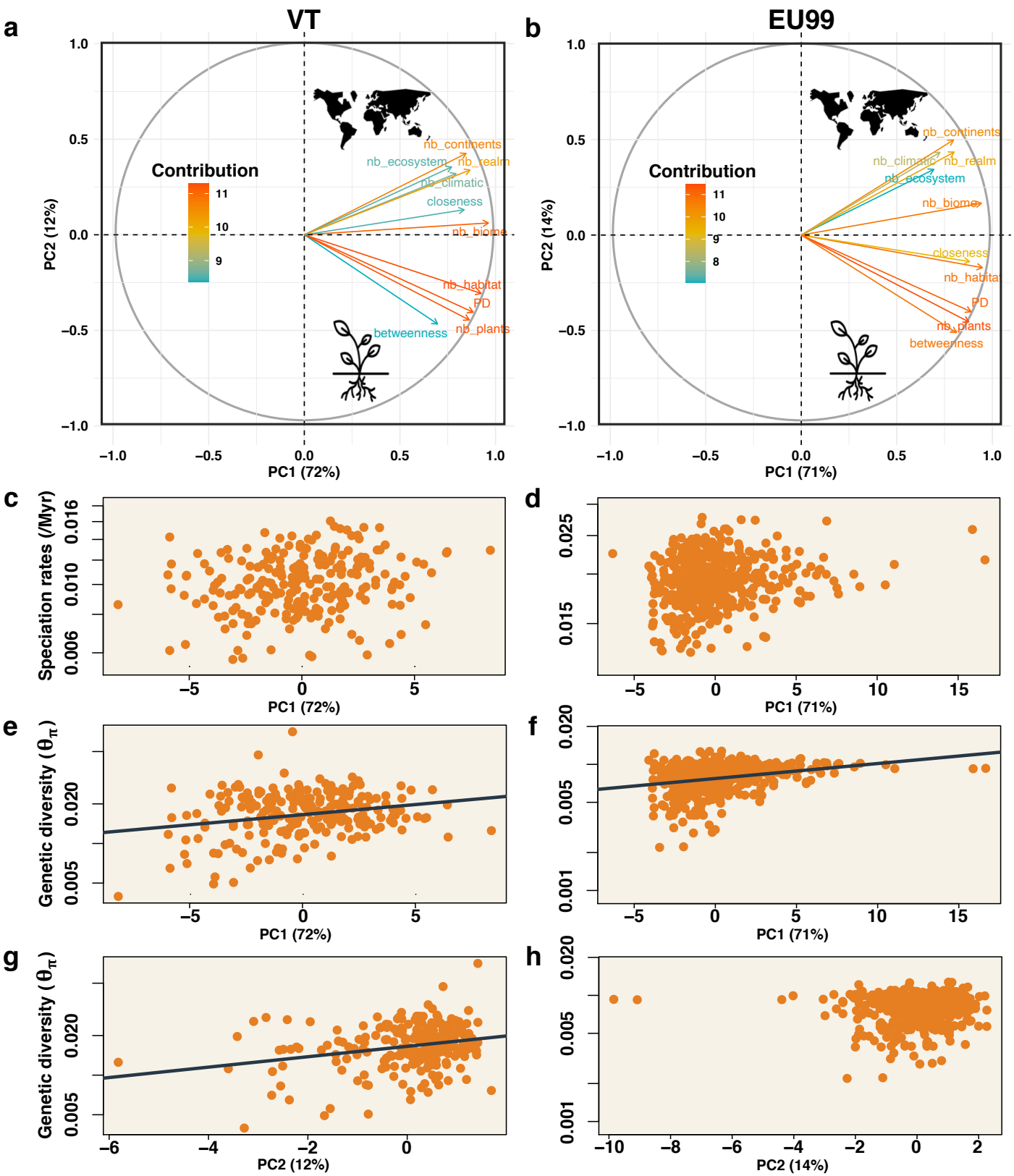
a
VT
b
EU99
Contribution
11
10
9
8
nb_continents
nb_ecosystem
nb_realm
nb_climatic
closeness
nb_biome
nb_habitat
PD
nb_plants
betweenness
PC1 (72%)
PC2 (12%)
PC1 (71%)
PC2 (14%)
c
d
e
f
g
h
Speciation rates (/Myr)
Genetic diversity (θ_π)

867